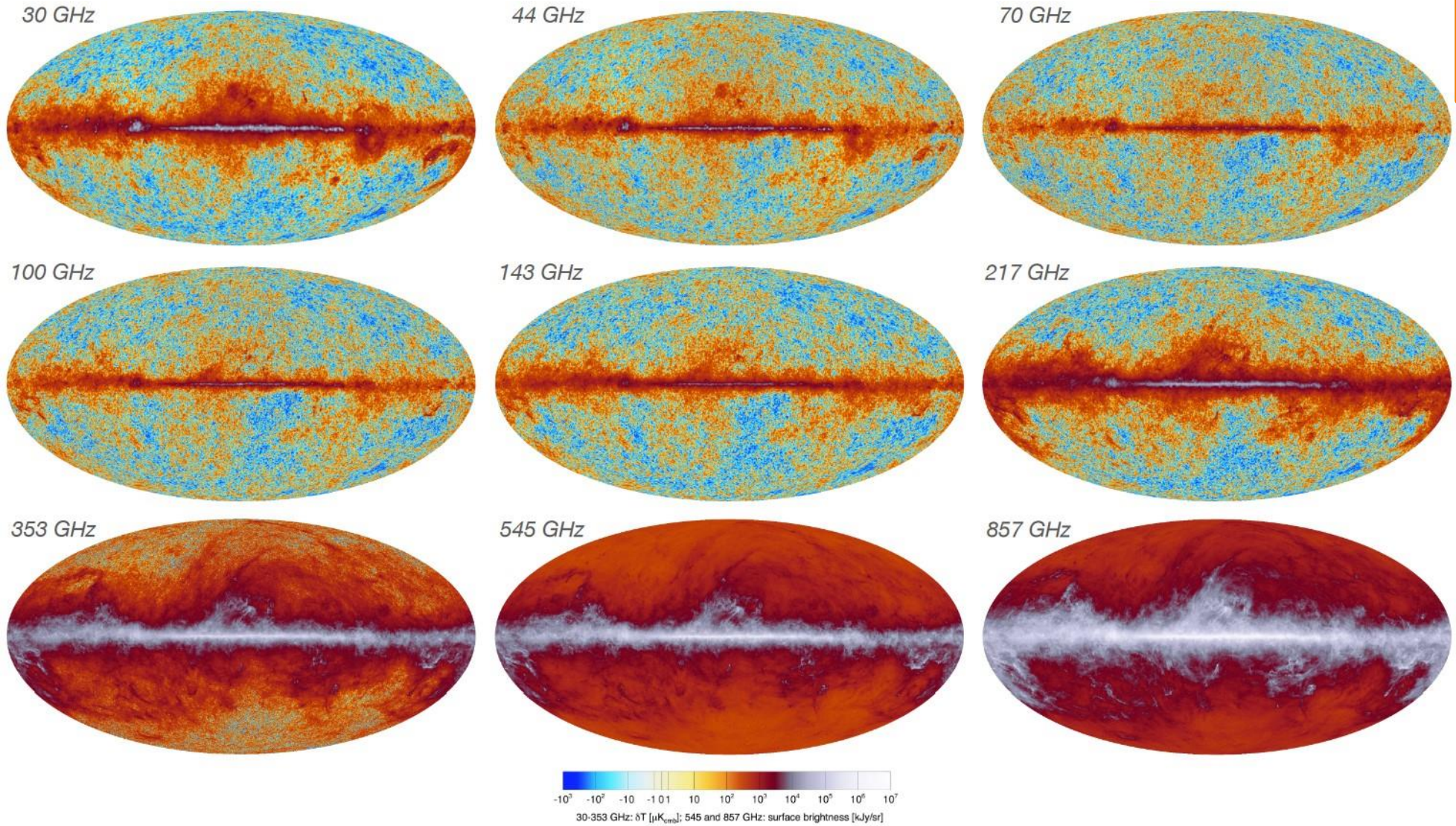


Pressure profiles of galaxy cluster from SPT and Planck observations.

F. OPPIZZI, H. BOURDIN, F. DE LUCA, P. MAZZOTTA
UNIVERSITÀ DEGLI STUDI DI ROMA 'TOR VERGATA'

PLANCK



- ❖ ESA satellite mission launched in 2009.
- ❖ Full sky maps of temperature and polarization with sub-Jansky sensitivity.
- ❖ 9 frequency bands from 30 to 857 GHz.
- ❖ Resolution <10 arcmin.
- ❖ 1000+ cluster detected via the Sunyaev-Zeldovich effect (SZ).

(Planck Collaboration 2020, A&A,641,A1, arXiv:1807.06205)

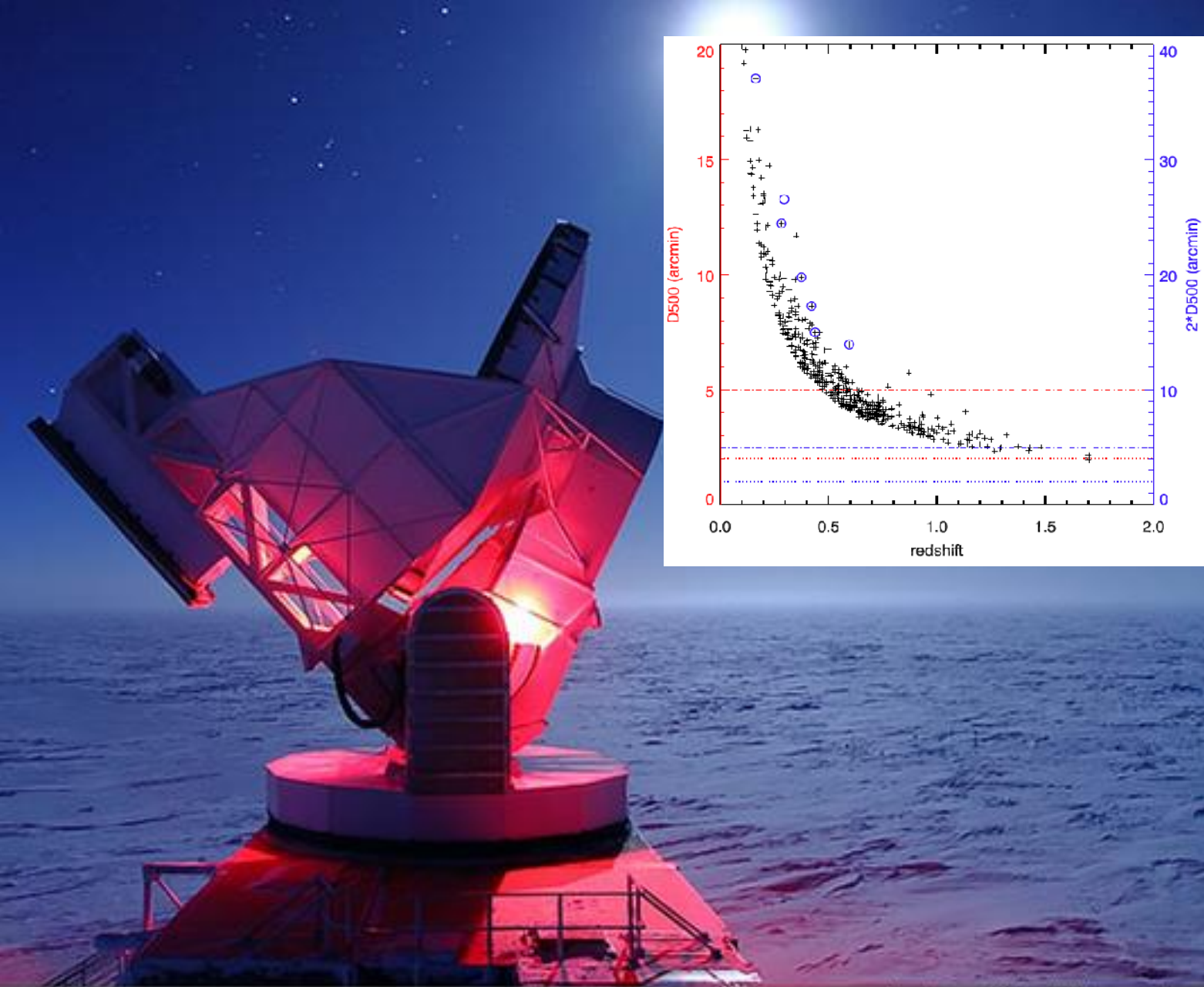


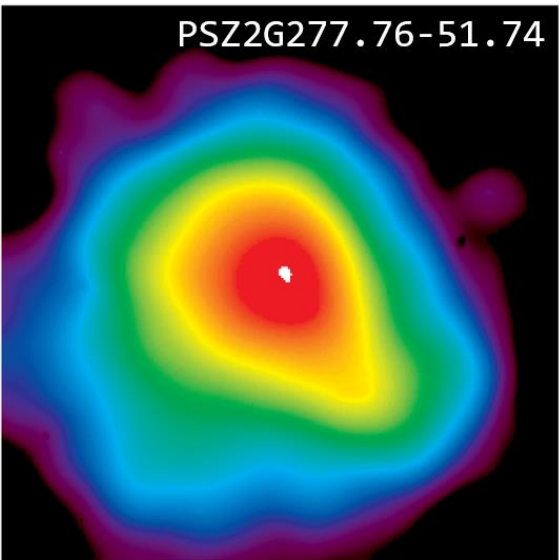
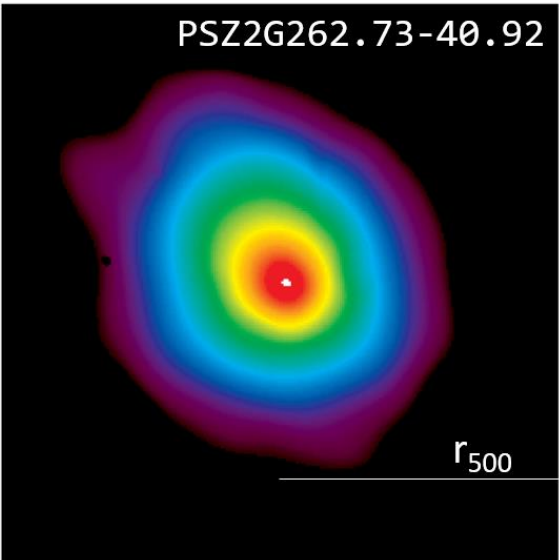
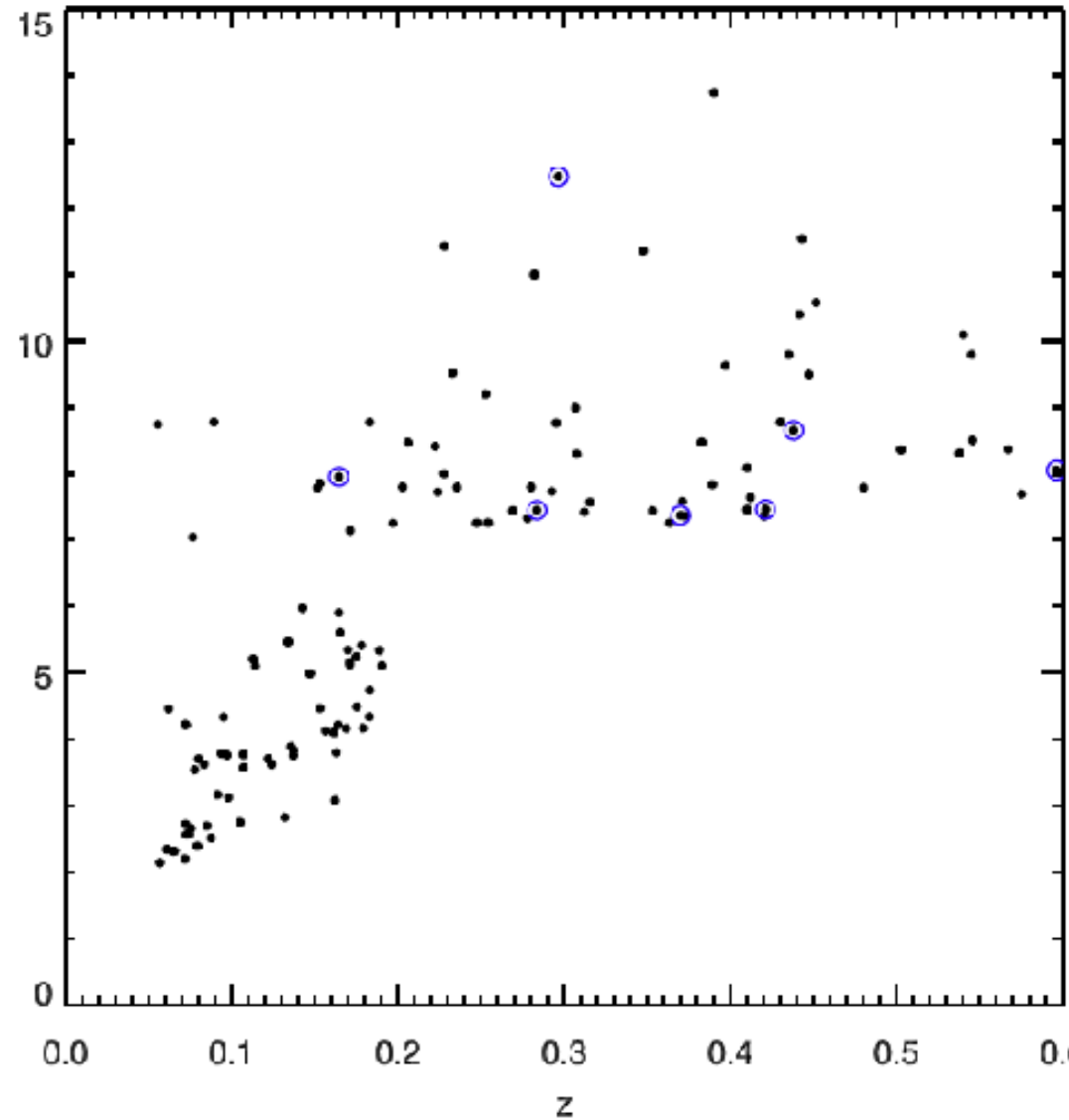
Photo Credit: Daniel Luong-Van

South Pole Telescope

- ❖ 3 channels: 95, 150, 220 GHz , resolution 1.75 arcmin.
- ❖ 2500 square-degree survey at high galactic latitude.
- ❖ 677 clusters candidates:
 - Nearly mass limited ($M_{500} > 2 \times 10^{14} M_{\odot}$).
 - Maximum redshift: 1.7.
- ❖ It allows to probe the redshift evolution of the cluster structure.
- ❖ SPT is sensitive to inner regions, Planck to the peripheries.

The Sample

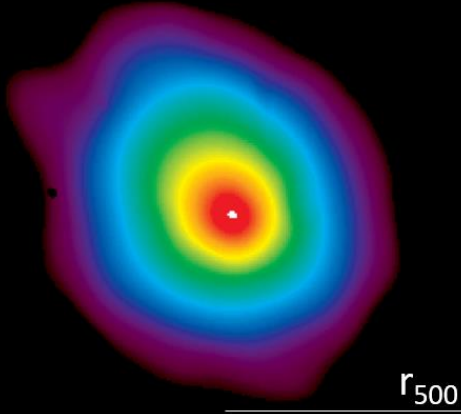
- ❖ We analyse a sub-sample of 6 clusters common to the SPT and CHEX-MATE catalogue. ([arXiv:2010.11972](https://arxiv.org/abs/2010.11972))
- ❖ We exploit the XMM data to validate our SZ pressure profile extraction algorithm.
- ❖ The comparison with X-ray spectroscopic data provides a powerful benchmark.
- ❖ We study the impact of sub-structure on the relation between SZ and X-ray profiles.



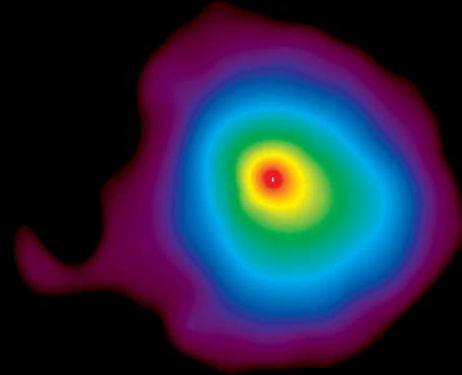
The Sample

- ❖ We analyse a sub-sample of 6 clusters common to the SPT and CHEX-MATE catalogue. ([arXiv:2010.11972](https://arxiv.org/abs/2010.11972))
- ❖ We exploit the XMM data to validate our SZ pressure profile extraction algorithm.
- ❖ The comparison with X-ray spectroscopic data provides a powerful benchmark.
- ❖ We study the impact of sub-structure on the relation between SZ and X-ray profiles.

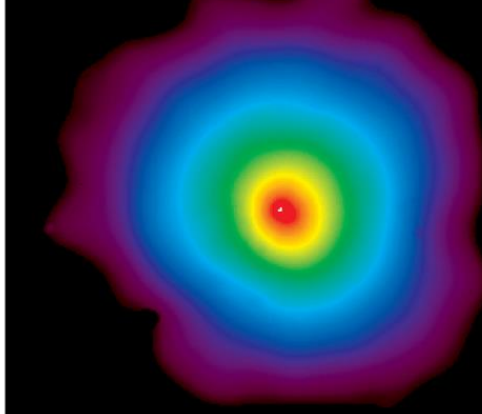
PSZ2G262.73-40.92



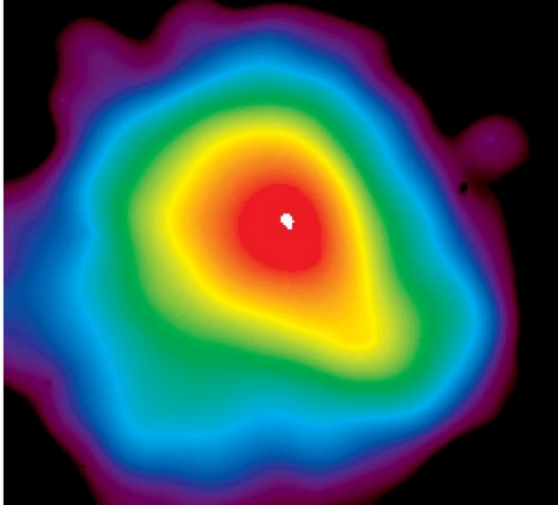
PSZ2G259.98-63.43



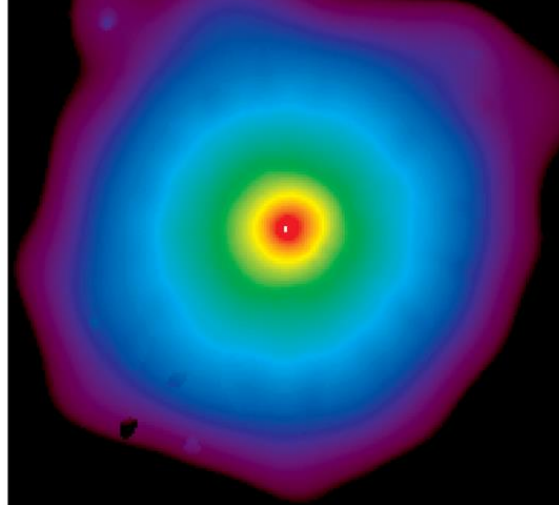
PSZ2G271.18-3095



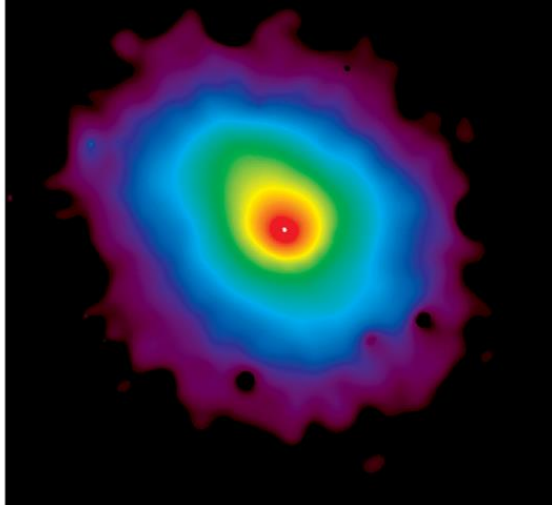
PSZ2G277.76-51.74



PSZ2G339.63-69.34



PSZ2G263.68-22.55

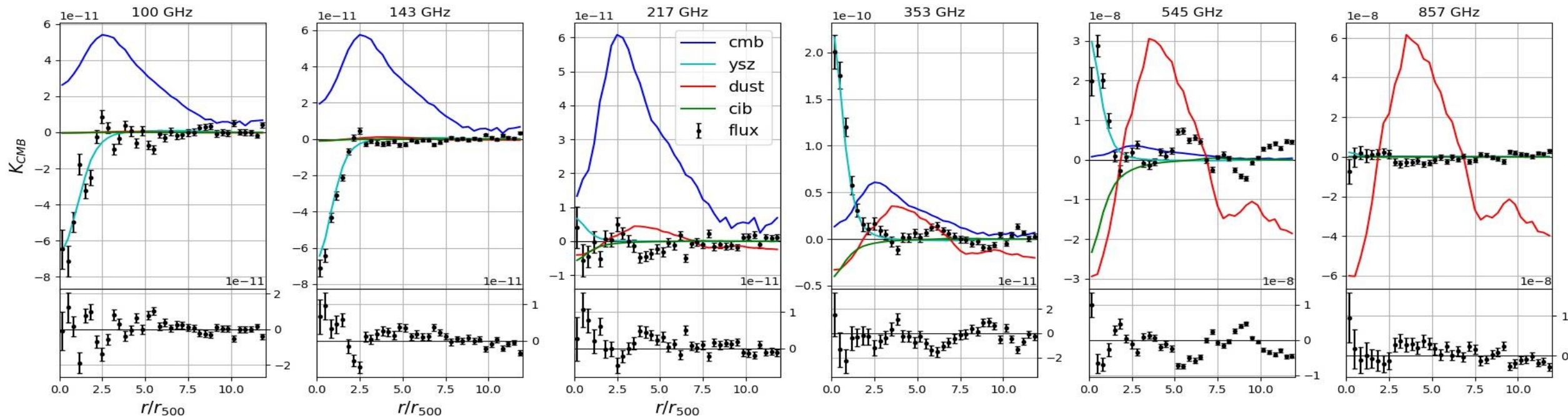


Component separation: Planck

(Bourdin et al. 2017, ApJ 843:72)

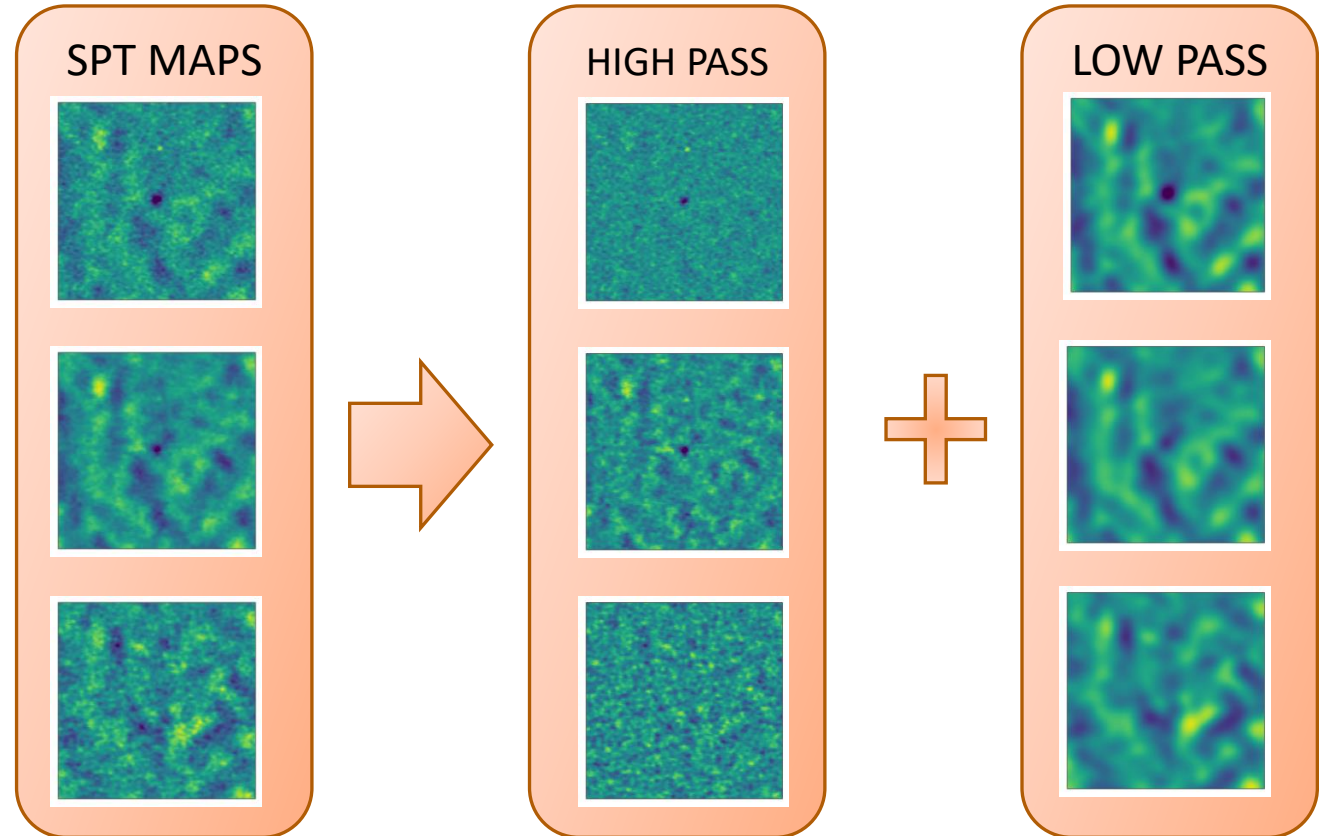
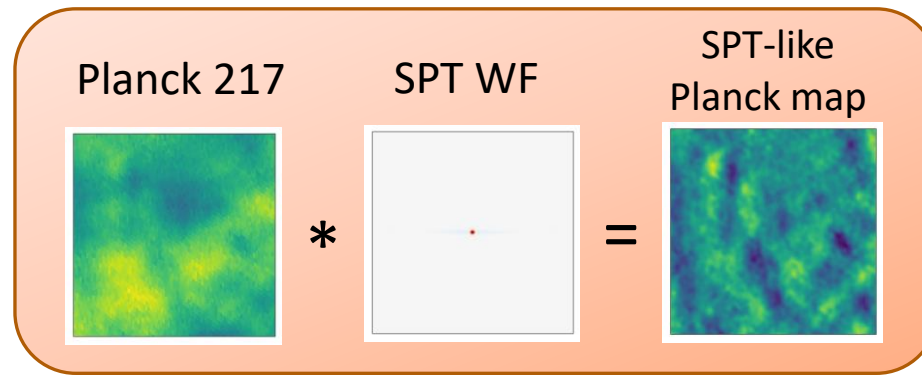
- ❖ Maps are high-pass filtered to remove large scale modes.
- ❖ 4 components fit:
 - cluster SZ signal.
 - Primary CMB anisotropies.
 - Galactic Thermal Dust (Meisner & Finkbeiner, 2005, ApJ, 798:88).
 - Intracluster Dust Correction.
- ❖ Cluster template gNFW profile (Nagai et al 2007) projected and convolved with the instrumental beams.
- ❖ The diffuse Components are recovered from the wavelets reconstruction of the 857GHz (Dust) and the 217GHz (CMB) channels.

psz2g259.98-63.43



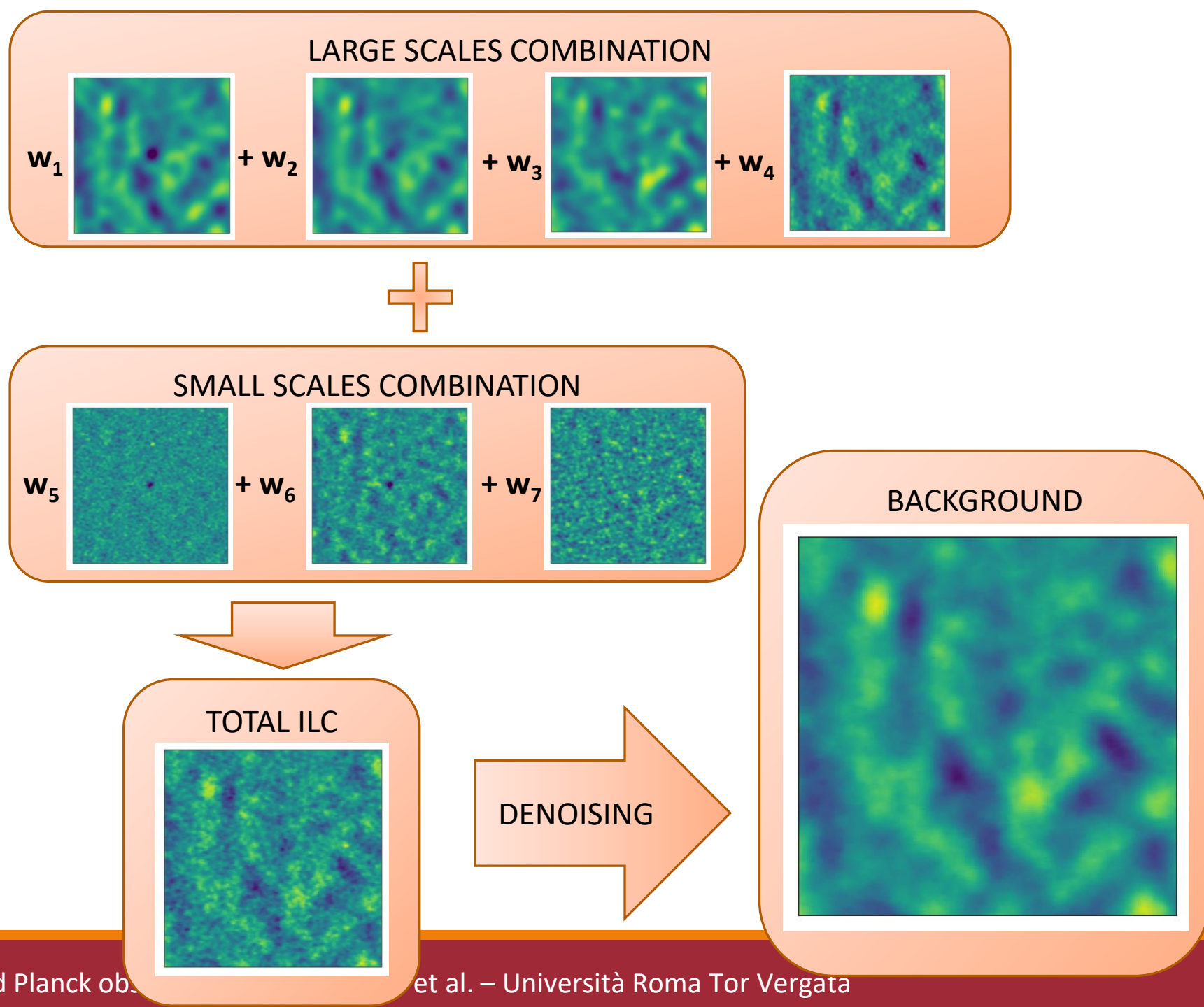
Component separation: SPT

- ❖ SPT maps are high-pass filtered due to the Filter Transfer Function.
- ❖ 220 GHz noise is very high.
- ❖ No significant dust contamination.
- ❖ To recover the background (CMB) in SPT we resort to a *Multiscale Internal Linear Combination*, including also the Planck 217GHz Channel.
- ❖ The weights minimize the CMB variance nulling the SZ component

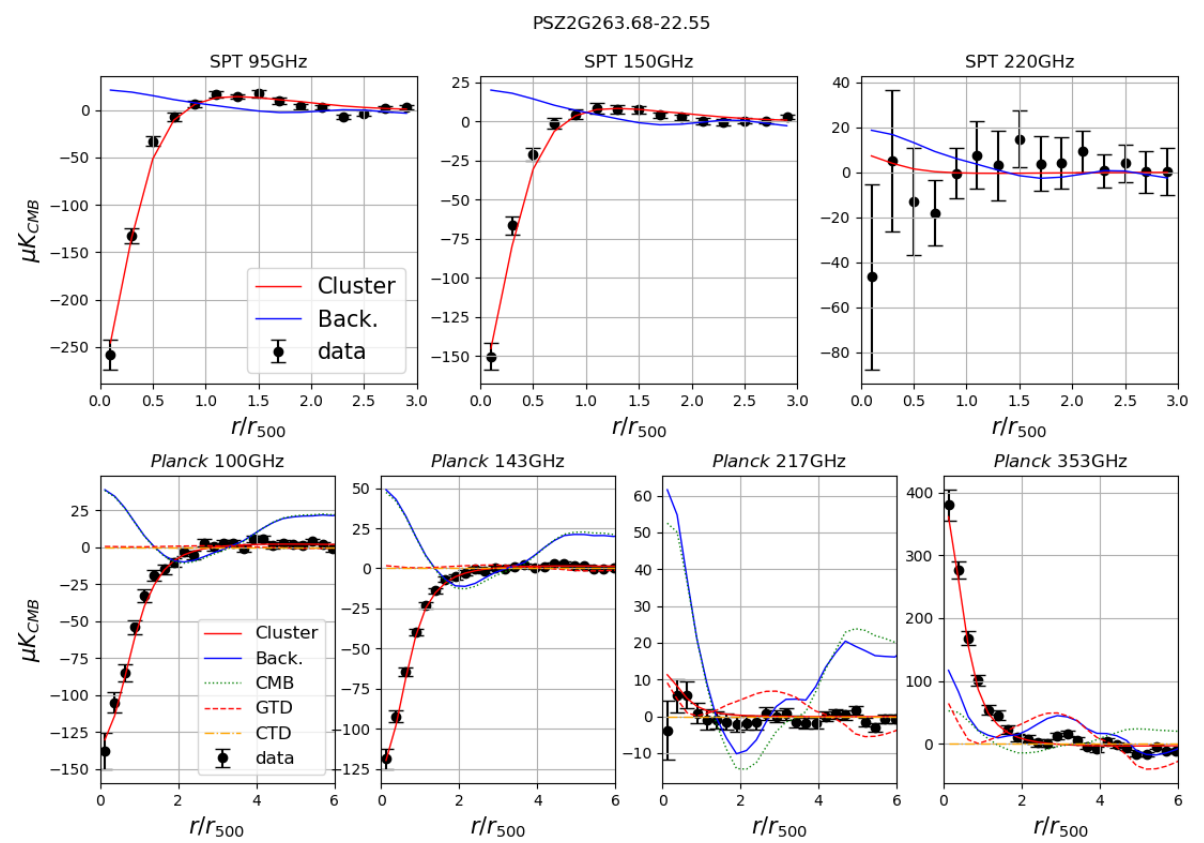
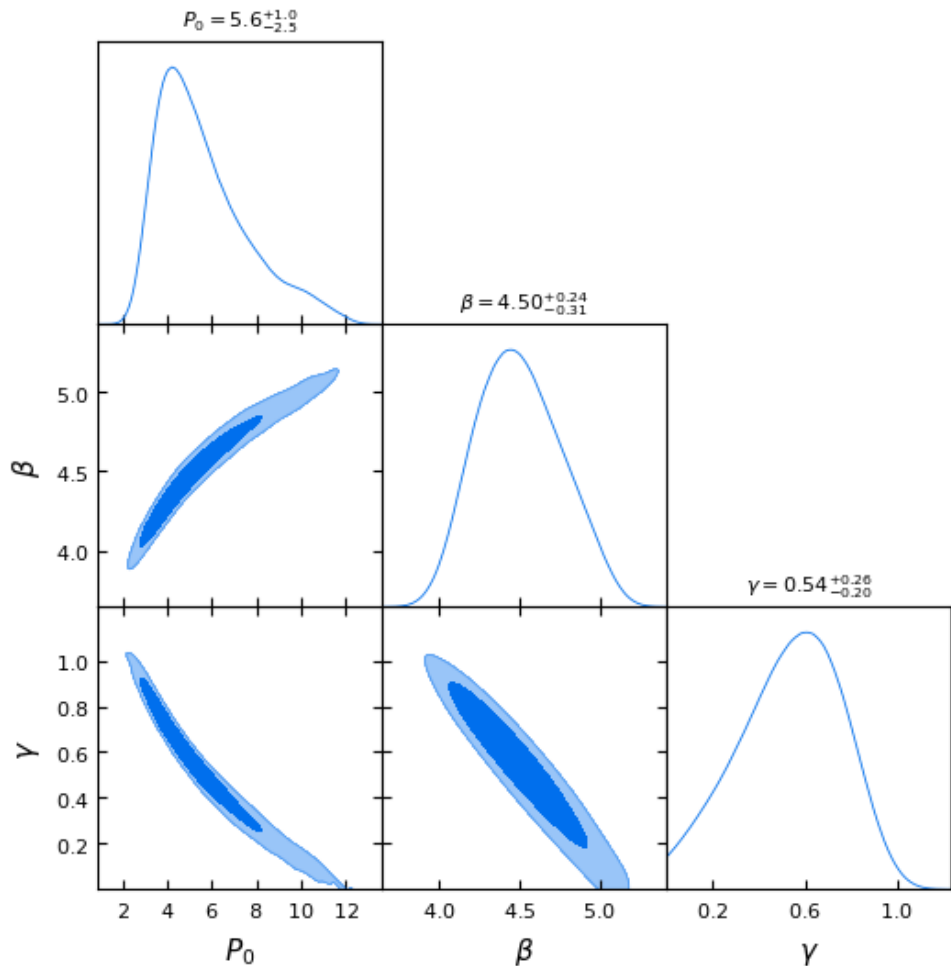


Component separation: SPT

- ❖ SPT maps are high-pass filtered due to the Filter Transfer Function.
- ❖ 220 GHz noise is very high.
- ❖ No significant dust contamination.
- ❖ To recover the background (CMB) in SPT we resort to a *Multiscale Internal Linear Combination*, including also the Planck 217GHz Channel.
- ❖ The weights maximize the CMB signal nulling the SZ component



SPT-Planck Joint fit



❖ We combine the cleaned maps in a joint fit of a gNFW profile.

❖ We use the 95, 150 GHz SPT channels and the 100, 143, 353 GHz from Planck HFI.

❖ Nagai profile with 3 free parameters:

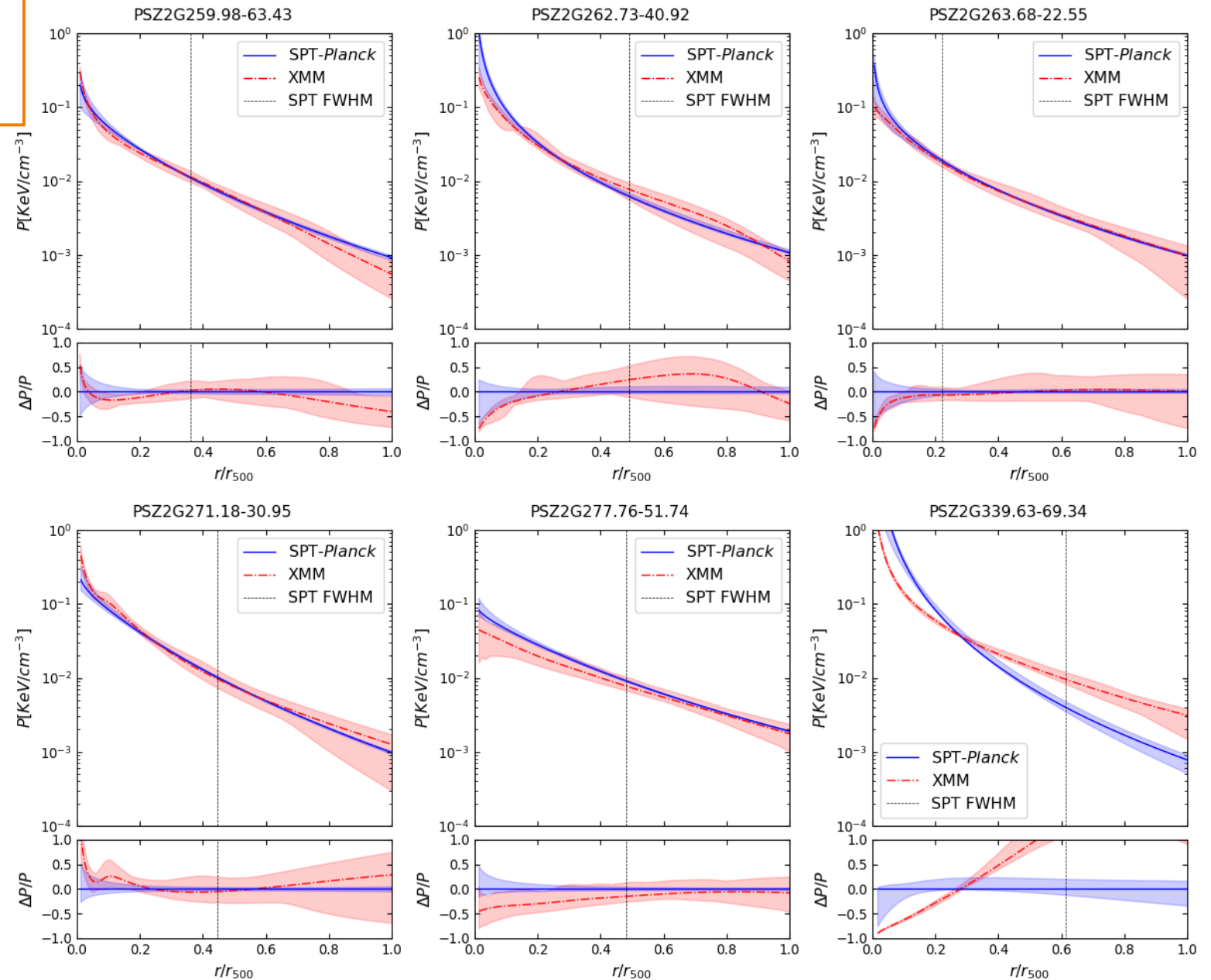
1. Amplitude P_0 .
2. 2 slopes: β for $r \gg r_{500}$, γ for $r \ll r_{500}$.
3. Intermediate slope and concentration fixed $\alpha = 1.051$, $c_{500} = 1.177$ (Arnaud et al., 2010).

$$P(r) = P_0 \frac{P_{500}}{x^\gamma (1 + x^\alpha)^{\frac{\beta - \gamma}{\alpha}}}$$

$$x = r c_{500} / r_{500}$$

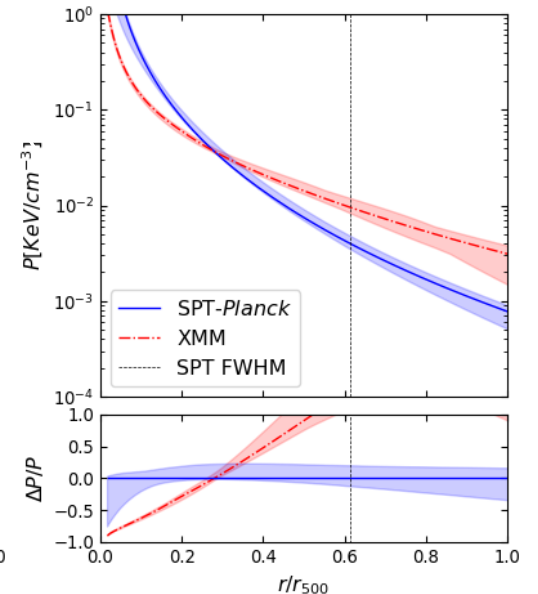
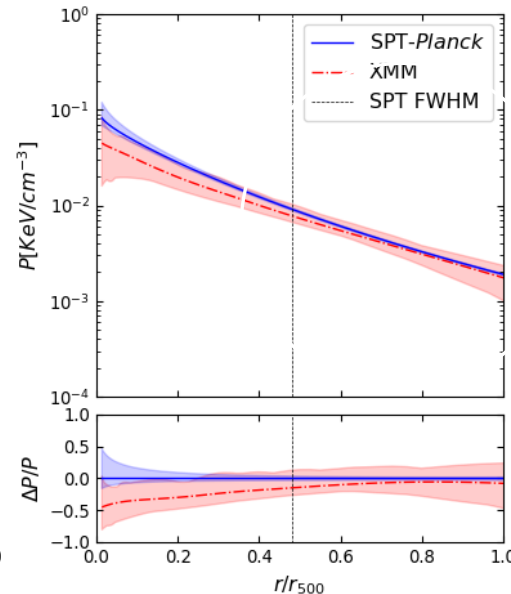
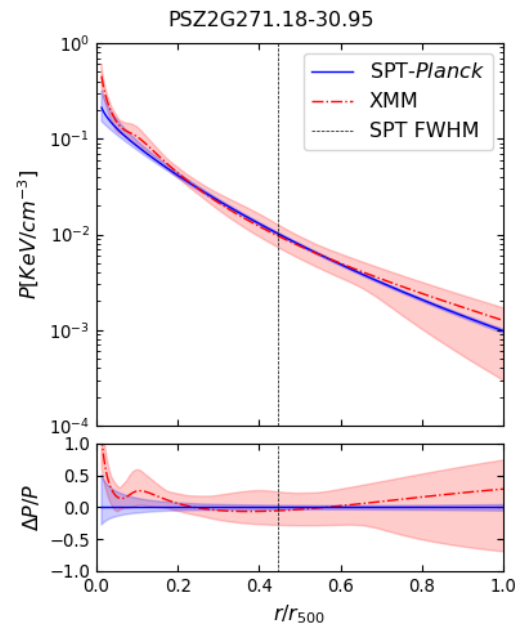
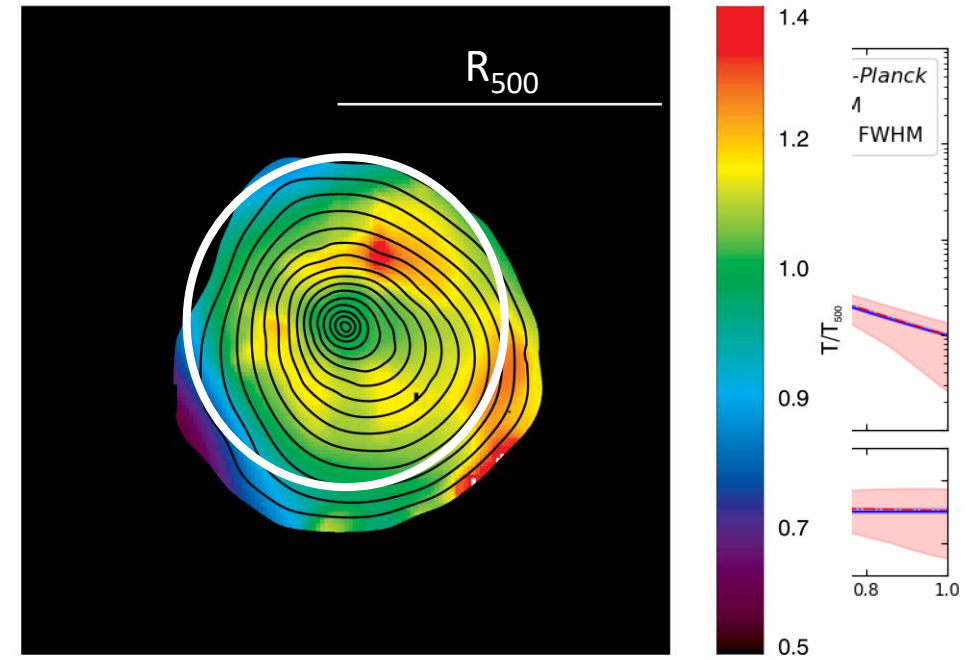
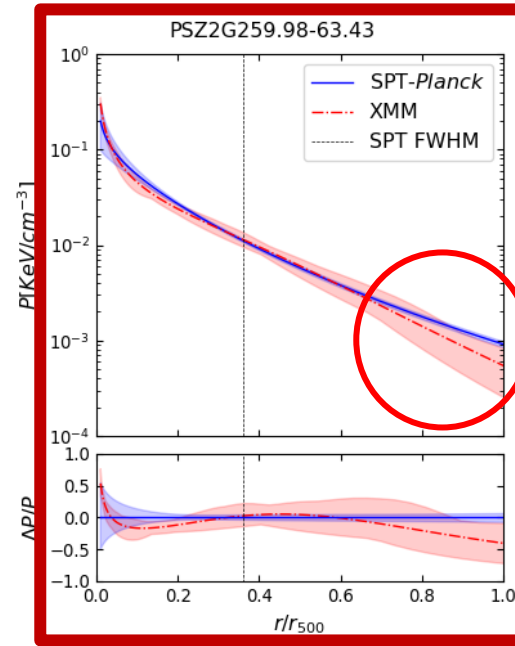
Profiles comparison

- ❖ The comparison with XMM profiles shows good agreement in the innermost regions.
- ❖ The agreement is higher in the cluster with regular shape.
- ❖ PSZ2G259.98-63.43 presents a slight deviation around r_{500} probably explained by the irregular shape.
- ❖ The Phoenix cluster (PSZ2G339.63-69.34) is contaminated by a strong AGN X-ray emission.



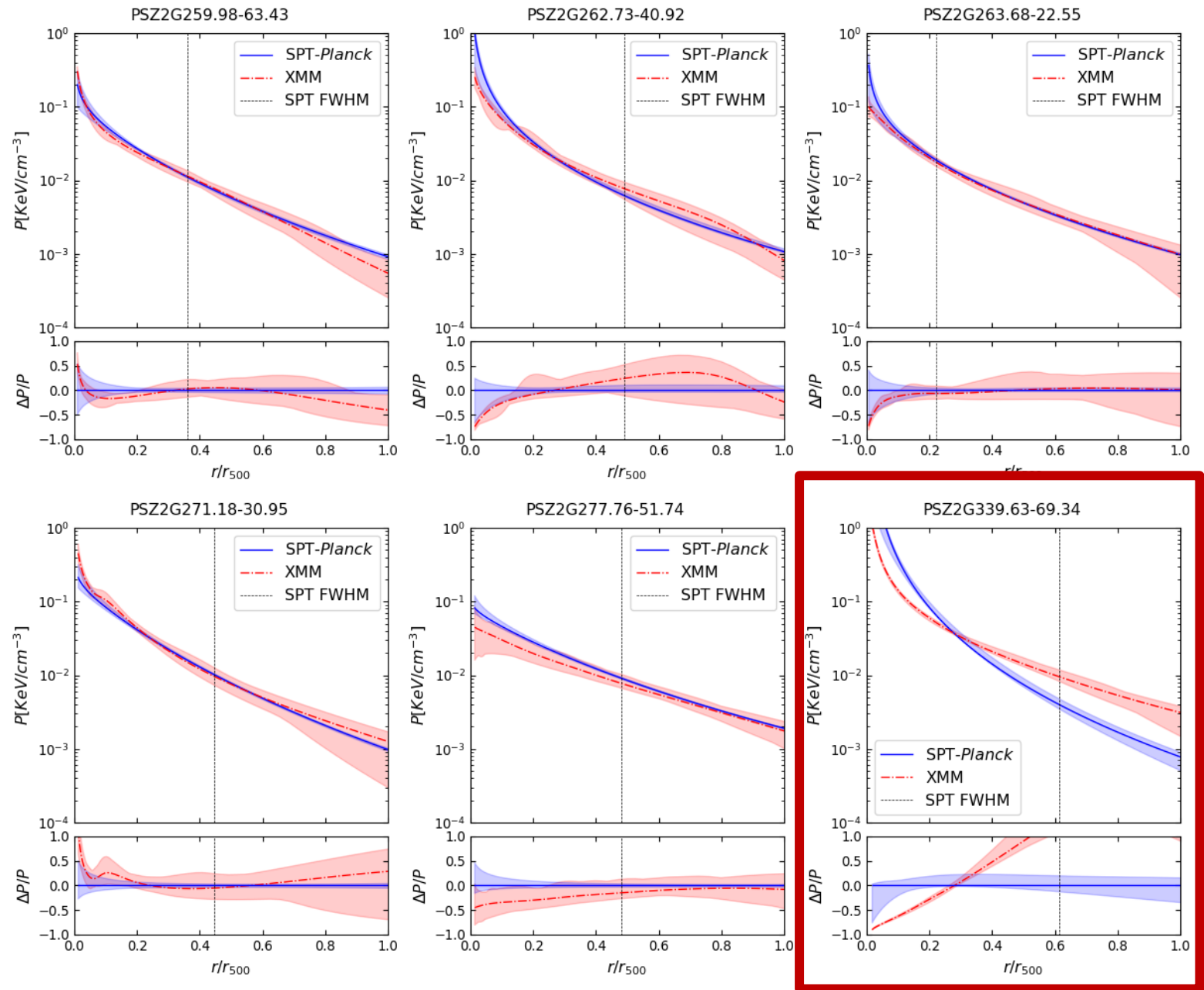
Profiles comparison

- ❖ The comparison with XMM profiles shows good agreement in the innermost regions.
- ❖ The agreement is higher in the cluster with regular shape.
- ❖ PSZ2G259.98-63.43 presents a slight deviation around r_{500} probably explained by the irregular shape.
- ❖ The Phoenix cluster (PSZ2G339.63-69.34) is contaminated by a strong AGN X-ray emission.



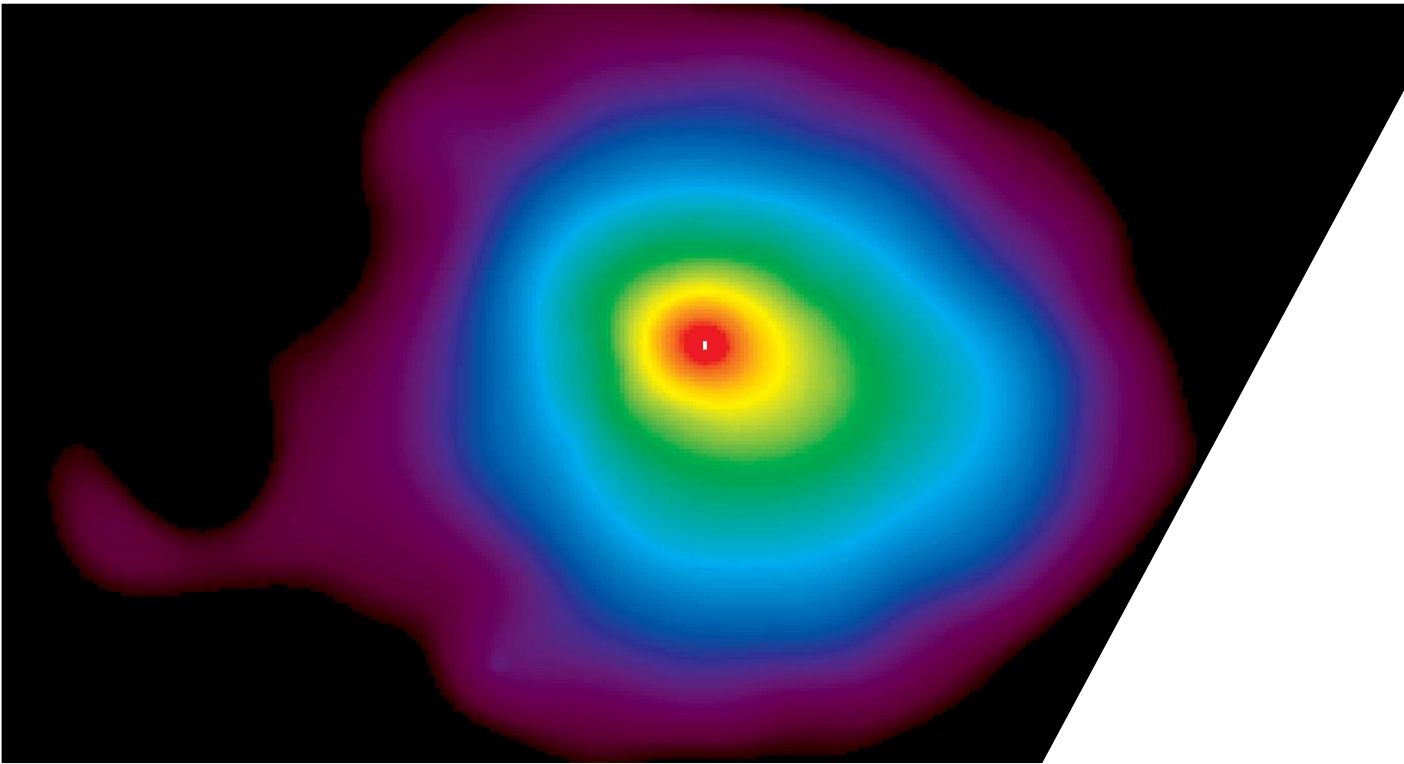
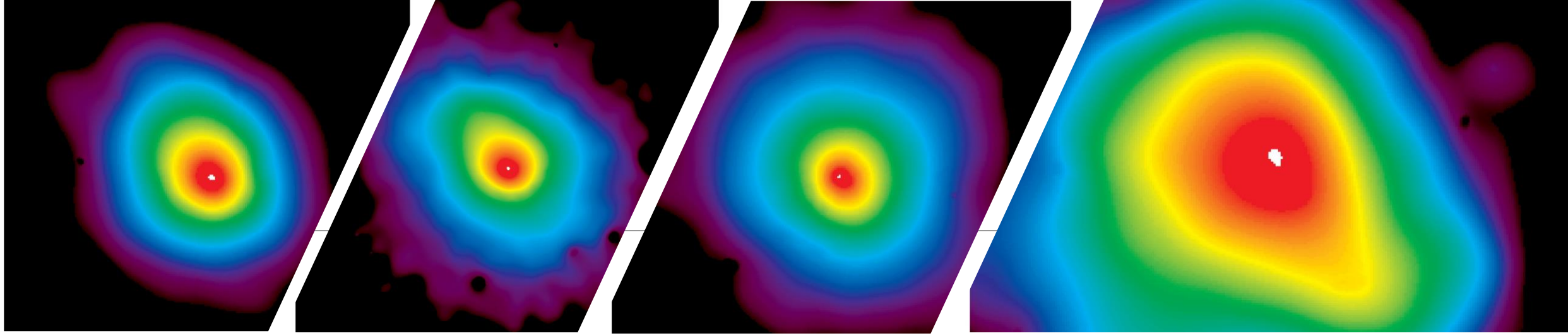
Profiles comparison

- ❖ The comparison with XMM profiles shows good agreement in the innermost regions.
- ❖ The agreement is higher in the cluster with regular shape.
- ❖ PSZ2G259.98-63.43 presents a slight deviation around r_{500} probably explained by the irregular shape.
- ❖ The Phoenix cluster (PSZ2G339.63-69.34) is contaminated by a strong AGN X-ray emission.



Conclusion and future works

- ❖ We develop a complete set of tools to extract cluster pressure profiles from the joint analysis of Planck and SPT data.
- ❖ Combining the datasets allows us to fit the profile from the inner to the outermost regions of the clusters.
- ❖ We implemented two specific pipelines for the component separation on SPT and Planck.
- ❖ The comparison with XMM data on a pilot sample overlapping the CHEX-MATE catalogue shows good agreement between the X-ray and millimetre data.
- ❖ We investigate the impact of irregularities in the cluster shape to explain potential discrepancies.
- ❖ We will extend the analysis to a larger part of the SPT catalogue.



Thank You!